The offloading model for dynein function: differential function of motor subunits

Wei-Lih Lee, Michelle A. Kaiser, and John A. Cooper

Department of Cell Biology and Physiology, Washington University School of Medicine, St. Louis, MO 63110

During mitosis in budding yeast, dynein moves the mitotic spindle into the mother-bud neck. We have proposed an offloading model to explain how dynein works. Dynein is targeted to the dynamic plus end of a cytoplasmic microtubule, offloads to the cortex, becomes anchored and activated, and then pulls on the microtubule. Here, we perform functional studies of dynein intermediate chain (IC) and light intermediate chain (LIC). IC/Pac11 and LIC/Dyn3 are both essential for dynein function, similar to the heavy chain (HC/Dyn1). IC and LIC are targeted to the distal plus ends of dynamic cytoplasmic microtubules, as is HC, and their targeting depends on HC. Targeting of HC to the plus end depends on IC, but not LIC. IC also localizes as stationary dots at the cell cortex, the presumed result of offloading in our model, as does HC, but not LIC. Localization of HC to cortical dots depends on both IC and LIC. Thus, the IC and LIC accessory chains have different but essential roles in dynein function, providing new insight into the offloading model.

Introduction

During mitosis in budding yeast, the mitotic spindle moves into the mother-bud neck via dynein-dependent sliding of cytoplasmic microtubules along the cortex of the bud (Adames and Cooper, 2000). We previously proposed an offloading model in which dynein is delivered by microtubule plus ends to the bud cortex, where dynein becomes anchored to generate forces for microtubule sliding (Lee et al., 2003). Our model was inspired by our discovery that the heavy chain of dynein, Dyn1, localizes to the distal plus ends of cytoplasmic microtubules as they grow and shrink. Furthermore, Dyn1 localizes to stationary dots at the cortex, which we proposed represent the end product of the offloading process.

Cytoplasmic dynein from vertebrates contains two heavy chains (HCs), two intermediate chains (ICs), two to four light intermediate chains (LICs), and four to five light chains (LCs) (see Table I in King et al., 2002). The HC contains the motor domain. The accessory chains are important for mediating the functions performed by HC. In *Caenorhabditis elegans* and cultured vertebrate cells, loss of IC or LIC function shows defects in cytoplasmic dynein function (Gaglio et al., 1997; Compton, 2000; Yoder and Han, 2001; Rusan et al., 2002).

In budding yeast, *PAC11* is proposed to encode a dynein IC based on sequence similarity with rat dynein IC (22.4% identity; Geiser et al., 1997). *pac11* was isolated as synthetic lethal with the kinesin gene *cin8* (Geiser et al., 1997). *pac11* mutations showed a binucleate phenotype comparable to that of *dyn1*, and Pac11 coimmunoprecipitated with Dyn1 (Kahana et al., 1998). Here, we characterize Pac11 further and confirm its identity as dynein IC. In addition, we identified a dynein LIC, Ymr299c, in a genome-wide screen for a dynein-like nuclear migration phenotype. Ymr299c was previously identified in a genome-wide screen for *kar9* synthetic lethality (Tong et al., 2004). We show that Ymr299c biochemically associates with Dyn1, colocalizes with Dyn1 in cells, and is necessary for dynein function. Based on our results, we suggest naming *YMR299C* as *DYN3*.

Having identified Dyn3 and Pac11 as accessory chains of the dynein complex, we examined their role in dynein targeting and protein stability. Remarkably, some properties of Dyn3 are completely different from those of Pac11, revealing differential functions for the accessory chains. The results provide new insights into the offloading model for the function of dynein.

Results and discussion

Identification of *DYN3*

We screened all viable haploid null mutants in the Research Genetics collection for dynein function by a nuclear segregation cold assay (see Materials and methods). *ymr299c*Δ showed a high level of binucleate cells characteristic of dynein pathway null mutants.

Correspondence to John A. Cooper: jcooper@wustl.edu

Abbreviations used in this paper: 3D, three dimensional; HC, heavy chain; IC, intermediate chain; LIC, light intermediate chain.

The online version of this article includes supplemental material.

The Journal of Cell Biology, Vol. 168, No. 2, January 17, 2005 201–207
http://www.jcb.org/cgi/doi/10.1083/jcb.200407036

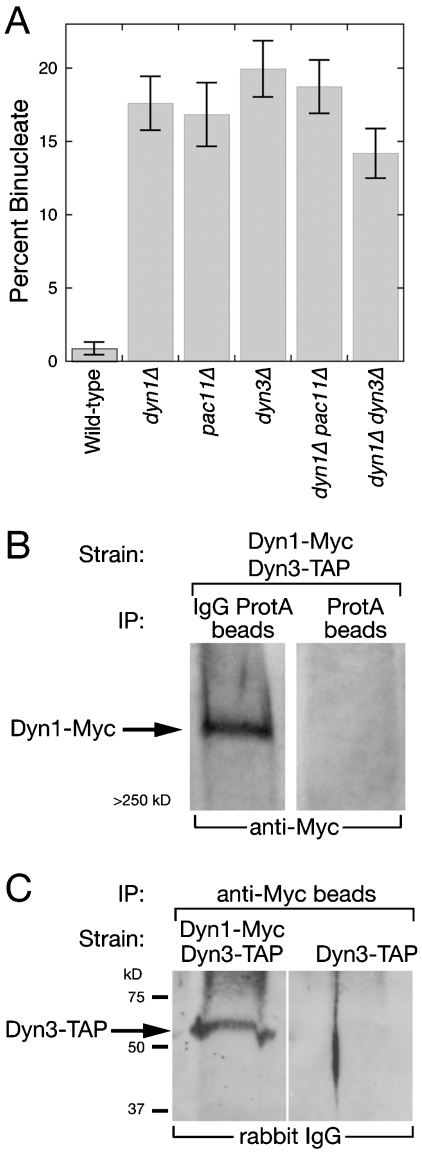

Figure 1. **Dyn3 is required for dynein function and coimmunoprecipitates with Dyn1.** (A) The percentage of cells with two nuclei in the mother in a nuclear segregation cold assay is plotted for the indicated strains. Error bars represent standard error of proportion (n = 300–500 cells for each strain). $P > 0.4$ for *dyn1*Δ to *dyn3*Δ; $P > 0.1$ for *dyn1*Δ *dyn3*Δ to *dyn1*Δ; $P > 0.02$ for *dyn1*Δ *dyn3*Δ to *dyn3*Δ; $P > 0.5$ for *dyn1*Δ to *pac11*Δ; $P > 0.5$ for *dyn1*Δ *pac11*Δ to *dyn1*Δ; $P > 0.2$ for *dyn1*Δ *pac11*Δ to *pac11*Δ. (B) An extract from cells expressing Myc-tagged Dyn1 and TAP-tagged Dyn3 was incubated with IgG/protein A beads, and the bound proteins were immunoblotted with anti-Myc. Dyn1-Myc coprecipitated with IgG/protein A beads, but not with control beads carrying protein A without IgG. (C) A similar cell extract as in B was incubated with anti-Myc beads. Bound proteins were immunoblotted with rabbit IgG to detect the TAP tag. Dyn3-TAP coprecipitated from a Dyn1-Myc extract, but not from the control extract in which Dyn1 was not tagged.

BLAST searches using Ymr299c, hereafter referred to as Dyn3, revealed similarity with cytoplasmic dynein LICs from fly, worm, and mammals. The level of similarity between Dyn3 and dynein LICs is low. Overall, Dyn3 has 4.4% identity and 17% similarity when aligned with *Drosophila*, *C. elegans*, and human LIC proteins (Fig. S1 A, available at http://www.jcb.org/cgi/content/full/jcb.200407036/DC1). A region in the middle of Dyn3 (residues 162–246) contains most of the homology with other LICs (13% identities and 32% similarities within this region). Additionally, Dyn3 does not have the conserved P-loop motif found in the NH_2-terminal region of *Drosophila* (residues 56–63), worm (residues 53–60), and mammalian (residues 61–68) LICs. We found Dyn3-like sequences in four yeast species closely related to *Saccharomyces cerevisiae*. Phylogenetic analysis showed that the yeast Dyn3 sequences do not group with the LIC clusters of cytoplasmic or axonemal dyneins from other organisms (Fig. S1 B). Thus, we conclude that Dyn3 is a distant homologue of dynein LIC, and further characterize its role as an LIC below.

Function of Dyn3 and Pac11

We tested whether Dyn3 is necessary for dynein function by comparing the cold binucleate phenotype of a *dyn3*Δ mutant with that of a *dyn1*Δ mutant and a *dyn1*Δ *dyn3*Δ double mutant. The levels of binucleate cells in all three strains were quantitatively the same (Fig. 1 A). Thus, the functional consequences of the loss of Dyn3 are equivalent to the loss of Dyn1, and loss of both proteins is no worse than the loss of either one; therefore, Dyn3 is an essential component of the dynein pathway.

Deletion of *DYN1* is nearly lethal when combined with deletion of genes in the Kar9 pathway (Miller and Rose, 1998; Lee et al., 1999; Miller et al., 1999), which acts before the dynein pathway to move the nucleus near the neck in wild-type cells. To further test whether Dyn3 functions like Dyn1, we crossed a *dyn3*Δ strain with the Kar9 pathway mutants *bim1*Δ and *kar9*Δ. Tetrad analyses revealed that all *dyn3*Δ *bim1*Δ and *dyn3*Δ *kar9*Δ double-mutant progeny form very small colonies (Table I). They exhibit a severe growth defect when compared with wild type or parental single mutants, indicating a strong synthetic interaction of *dyn3*Δ with *bim1*Δ and *kar9*Δ. *dyn3*Δ *bim1*Δ colonies were even smaller than those of *dyn3*Δ *kar9*Δ, visible only under a dissection microscope after 4–5 d. No synthetic effect on growth was observed for double mutants of *dyn3*Δ with mutations in the dynein pathway (*dyn1*Δ and *num1*Δ; Table I). In positive control crosses, we found essentially identical synthetic interactions for double mutants of *dyn1*Δ with *bim1*Δ or *kar9*Δ (Table I). We conclude that Dyn3 is absolutely required for dynein function in nuclear migration.

Additionally, we tested whether IC/Pac11 is necessary for dynein function using the same genetic analysis described for LIC/Dyn3. Results for *pac11*Δ were similar to those for *dyn3*Δ (Fig. 1 A and Table I), indicating that Pac11 is also absolutely required for dynein function in nuclear migration.

Biochemical analysis: association of LIC/Dyn3 with HC/Dyn1

IC/Pac11 is known to associate with HC/Dyn1 (Kahana et al., 1998), as expected for an IC. We asked whether LIC/Dyn3 also exists in a complex with HC/Dyn1. We tagged *DYN3* with TAP and *DYN1* with Myc, by integration at the 3′ end of the respective chromosomal loci. Haploid strains with these fusion proteins as their only source of Dyn3 or Dyn1 were normal in the nuclear segregation cold assay, indicating full functionality (unpublished data).

Table I. **Synthetic effect of *dyn3*Δ or *pac11*Δ combined with Kar9 or dynein pathway mutations**

Double-mutant combination	Total number of predicted double mutants analyzed	Double mutants with normal colony size	Double mutants with small but visible colony size	Double mutants with small colony visible only under microscope	Appearance[a] of double mutants under microscope	Synthetic effect of double mutations
*dyn3*Δ *bim1*Δ	9	0	1	8	abnormal	+++
*dyn3*Δ *kar9*Δ	8	0	6	2	abnormal	++
*dyn3*Δ *dyn1*Δ	14	14	0	0	normal	–
*dyn3*Δ *num1*Δ	7	7	0	0	normal	–
*pac11*Δ *bim1*Δ	8	0	2	6	abnormal	+++
*pac11*Δ *kar9*Δ	9	0	9	0	abnormal	++
*pac11*Δ *dyn1*Δ	6	6	0	0	normal	–
*pac11*Δ *num1*Δ	5	5	0	0	normal	–
*dyn1*Δ *bim1*Δ	11	0	1	10	abnormal	+++
*dyn1*Δ *kar9*Δ	12	0	12	0	abnormal	++

Tetrad analysis was performed on heterozygous diploids. Double-mutant progeny were scored for colony size and morphology after 4–5 d incubation at 30°C on rich media.
[a]abnormal = elongated, swollen, irregular shape, and/or lysed appearance.

Immunoprecipitation of Dyn3-TAP and immunoblotting with anti-Myc revealed association of Dyn3 with Dyn1 (Fig. 1 B). Control beads not able to bind TAP gave a negative result. Conversely, immunoprecipitated Dyn1-Myc contained Dyn3-TAP. Dyn3-TAP was not precipitated from a control extract in which Dyn1 was not tagged (Fig. 1 C). Therefore, Dyn3 and Dyn1 are physically associated, consistent with Dyn3 being the LIC of the dynein motor complex.

Localization of Dyn3

Dyn1 is found at the distal plus ends of cytoplasmic microtubules (Lee et al., 2003; Sheeman et al., 2003) and in stationary dots at the cell cortex, which presumably represent the end product of offloading (Lee et al., 2003). To examine whether Dyn3 has the same localization, we tagged the chromosomal copy of *DYN3* at its 3′ end with 3YFP. The fusion gene is functional because a haploid strain with Dyn3-3YFP as the only form of Dyn3 had wild-type levels of binucleate cells in the nuclear segregation cold assay (unpublished data).

We observed Dyn3-3YFP localized to motile dots in the cytoplasm, not at the cortex as described in a previous report (Tong et al., 2004). The majority of cells contained one motile dot, and the number of dots per cell varied from zero to three. Dyn3-3YFP motile dots were observed in the bud and mother, and they colocalized with the plus ends of cytoplasmic microtubules (Fig. 2). Dyn3-3YFP dots moved through the cytoplasm toward and away from the cell cortex (Video 1, available at http://www.jcb.org/cgi/content/full/jcb.200407036/DC1), and were never stationary even when they encountered the cortex, with a 10-s image time interval.

The absence of stationary cortical dots for Dyn3 is a striking contrast with respect to Dyn1. We used three-dimensional (3D) image reconstructions as an additional approach to look for dots of dynein at the cortex. Full thickness stacks of confocal sections (see Materials and methods) were collected from single living cells. As we reported previously (Lee et al., 2003), Dyn1 localized to dots at the cell cortex, predominantly in the mothers of budding cells (mean 3.8 dots per mother cortex, range 2–6, $n = 11$ cells; Fig. 3 C; Videos 5 and 6). In the bud, cortical dots of Dyn1 were far less common. When present, they were found in large budded cells, where the mitotic spindle had moved into the neck (Fig. 4). Unbudded cells also contained dots of Dyn1 at the cortex (mean 3 per cell, range 1–5, $n = 9$). In contrast, for Dyn3-3YFP cells, 3D image reconstructions did not reveal any dots at the cortex of budded or unbudded cells (Fig. 3 A; Video 3), confirming the lack of stationary cortical dots in the movie analysis above. We conclude that Dyn1 and Dyn3 have overlapping but differential localizations.

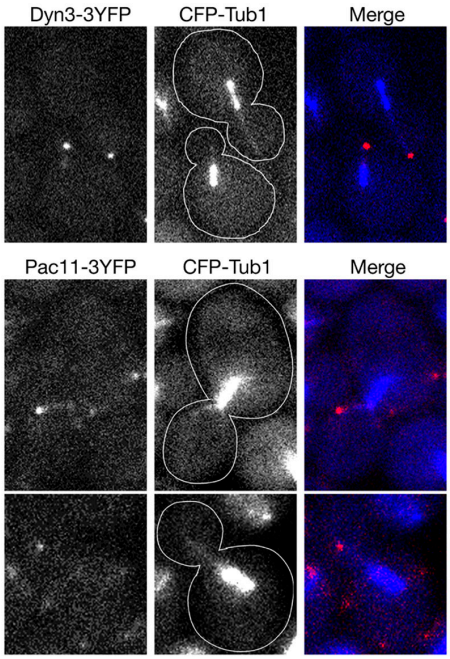

Figure 2. **Localization of Dyn3-3YFP and Pac11-3YFP.** (Top row) Dyn3-3YFP and CFP-Tub1 wide-field fluorescence images of wild-type cells. Dyn3-3YFP is observed in the cytoplasm as dots moving toward and away from the bud (see Video 1, available at http://www.jcb.org/cgi/content/full/jcb.200407036/DC1). The merged image shows cytoplasmic Dyn3-3YFP dots (red) at the distal ends of microtubules (blue). (Middle and bottom rows) Pac11-3YFP and CFP-Tub1 wide-field fluorescence images of wild-type cells. Pac11-3YFP is observed in the cytoplasm as motile dots and at the mother cortex as stationary dots (see Video 2), similar to what was observed for Dyn1-3GFP (Lee et al., 2003). The merged image shows Pac11-3YFP dots (red) at the distal ends of microtubules (blue) and the mother cortex.

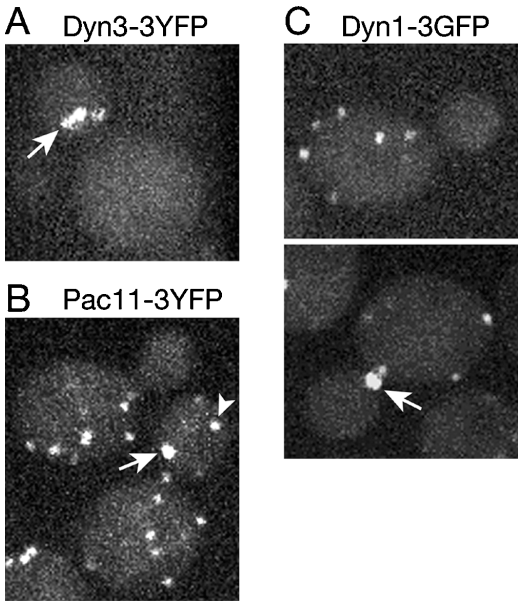

Figure 3. **2D projections from 3D image reconstructions of Dyn3-3YFP, Pac11-3YFP, and Dyn1-3GFP in living wild-type cells.** Rotating 3D images are shown as videos in the online supplemental materials (available at http://www.jcb.org/cgi/content/full/jcb.200407036/DC1). (A) Dyn3-3YFP is absent from the cortex (see Video 3 for rotating 3D image). The Dyn3-3YFP dot at the distal end of a microtubule moved during Z-collection, causing it to appear spread out in the bud cytoplasm arrow. (B and C) Pac11-3YFP and Dyn1-3GFP are observed as dots at the cortex, predominantly in the mother (dots in the bud are at microtubule ends arrows, and occasionally at the cortex in large buds arrowhead; also see Fig. 4). See Videos 4–6.

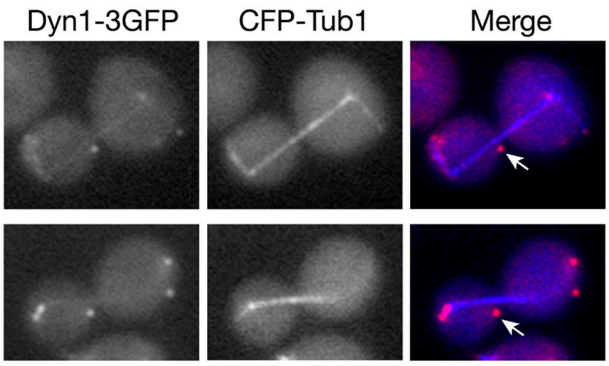

Figure 4. **Dyn1-3GFP at the cortex of large buds.** Dyn1-3GFP (red) and CFP-Tub1 (blue) wide-field fluorescence images of wild-type cells, showing Dyn1-3GFP dots at the bud cortex (arrows) of large budded cells in which the mitotic spindle had moved into the neck. These dots are not at the distal ends of cytoplasmic microtubules.

The level of Dyn1 at the microtubule plus end is enhanced in cells lacking dynactin or the cortical attachment protein Num1, which is interpreted to reflect accumulation due to the absence of offloading in our model (Lee et al., 2003). Also, the targeting of Dyn1 to the microtubule end is reduced in cells lacking the lissencephaly protein LIS1/Pac1 or CLIP170/Bik1 (Lee et al., 2003; Sheeman et al., 2003). We asked if Dyn3 at the plus end behaved in a similar manner. In cells lacking a dynactin component, Arp1 or p150Glued/Nip100, or the cortical attachment protein Num1, the fluorescence intensity of Dyn3-3YFP cytoplasmic dots was increased (Table II). In addition, the fluorescence intensity of Dyn3-3YFP dots was reduced in *pac1*Δ and *bik1*Δ mutants (Table II). Thus, Dyn3 resembles Dyn1 in these respects, consistent with the LIC of the dynein complex being targeted to plus ends and accumulating when offloading fails to occur.

Localization of Pac11

We asked whether the IC Pac11 localizes like the HC Dyn1 or the LIC Dyn3. We constructed a strain expressing Pac11-3YFP by integrating 3YFP at the 3′ end of the chromosomal *PAC11* gene. This strain had wild-type levels of binucleate cells in the nuclear segregation cold assay, indicating that the fusion protein functions when expressed from the endogenous promoter (unpublished data). We observed Pac11-3YFP as motile dots at the plus ends of cytoplasmic microtubules, as seen for Dyn1 and Dyn3 (Fig. 2). When tagged with the same 3YFP, the relative fluorescence intensity of Dyn1 to Pac11 to Dyn3 at the microtubule plus end was 7.7 ± 2.2 to 8.2 ± 0.9 to 10.2 ± 1.8 (arbitrary units mean ± standard error; $n = 5$ dots for Dyn1, $n = 5$ dots for Pac11, $n = 7$ dots for Dyn3). Thus, the subunits are present at plus ends in a 1:1:1 stoichiometry.

Movies of Pac11-3YFP cells revealed Pac11 in stationary dots at the cell cortex, predominantly of the mother (Video 2). Cortical dots of Pac11-3YFP were also seen in 3D image reconstructions of living cells (Fig. 3 B; Video 4). On average, the mother cortex of a budding cell had four to five Pac11-3YFP cortical dots (mean 4.6, range 2–8, $n = 10$ cells). In the bud, cortical dots of Pac11-3YFP were far less common, and they were only observed in large budded cells (Fig. 3 B, arrowhead). The cortex of unbudded cells also contained dots of Pac11-3YFP (mean 4.3 per cell, range 2–7, $n = 6$ cells). Thus, the localization of Pac11-3YFP is essentially identical to that of the HC Dyn1. We further examined the cortical dots of Pac11 using a strain coexpressing Pac11-3YFP and Dyn3-3CFP. We observed Pac11-3YFP dots at the cortex, but these cortical dots did not contain Dyn3-3CFP, as expected from analysis of Dyn3 localization above (Fig. S2 A, available at http://www.jcb.org/cgi/content/full/jcb.200407036/DC1). We conclude that the IC/Pac11 and LIC/Dyn3 are differentially localized, reflecting differential behavior at the cortex.

Differential roles of Pac11 and Dyn3 in dynein function

We asked whether Pac11 and Dyn3 are required for targeting of dynein HC/Dyn1 to the plus ends of microtubules. In *pac11*Δ cells, Dyn1-3GFP motile dots were either absent or very faint (Fig. 5 A; Video 7). Immunoblot analysis showed that the level of Dyn1 protein was reduced or absent in *pac11*Δ lysates, as compared with wild-type lysates (Fig. S2 B); thus, the loss of Dyn1-3GFP from the plus ends of microtubules was likely due to unstable protein. In contrast, in *dyn3*Δ cells, Dyn1-3GFP was seen as dots in the cytoplasm, that moved rapidly and sometimes formed linear streaks in the bud, a behavior characteristic of the plus ends of cytoplasmic microtubules (Fig. 5 A; Video 8). The fluorescence intensity of Dyn1-3GFP

Table II. **Relative fluorescence intensity of Dyn3-3YFP dots in isogenic wild-type and mutant strains**

Strains	Relative fluorescence intensity per Dyn3-3YFP dot
Wild-type	100
*arp1*Δ	160.0
*nip100*Δ	174.1
*num1*Δ	140.5
*pac1*Δ	55.4
*bik1*Δ	68.2

Wide-field fluorescence images were collected using the same microscope settings. The average corrected fluorescence per Dyn3-3YFP dot in a mutant was expressed as a percentage of that in wild type. $n = 100$ dots for each strain.

motile dots in *dyn3*Δ cells was similar to that in wild-type cells (unpublished data). We conclude that Dyn1 targeting to the plus ends of microtubules depends on Pac11 but not Dyn3, again revealing differential roles for the accessory chains.

The offloading model predicts that stationary cortical dots of dynein do not form when protein involved in offloading or anchoring of dynein is absent, as previously observed in cells lacking dynactin complex or the cortical attachment protein Num1 (Lee et al., 2003). Our observation that *dyn3*Δ mutant had a complete loss of dynein function (Fig. 1 A; Table I) but a normal Dyn1 localization at the plus end therefore predicts an absence of stationary cortical dots of dynein. As expected, no stationary cortical dots of Dyn1-3GFP were observed in *dyn3*Δ cells (Fig. 5 A; Video 8). Stationary cortical dots of Dyn1-3GFP were also absent in *pac11*Δ cells (Fig. 5 A; Video 7), as expected due to unstable Dyn1 protein.

We asked whether the localization of Pac11 and Dyn3 to the plus ends of microtubules depends on the HC Dyn1. In *dyn1*Δ cells, no localization of Pac11-3YFP or Dyn3-3YFP to motile dots in the cytoplasm was observed (Fig. 5 B). In addition, stationary cortical dots of Pac11-3YFP were not observed. Immunoblot analyses of Pac11 (Reck-Peterson and Vale, 2004) and Dyn3 (Fig. S2 C) proteins in *dyn1*Δ cell lysates showed that the level of each protein was the same as in wild-type cell lysates; thus, the loss of Pac11 and Dyn3 from the plus ends of microtubules is due to a loss in protein targeting, not stability. We conclude that Dyn1 is required for Pac11 and Dyn3 localization.

Conclusions: mechanism of dynein function

In our offloading model, dynein is released from the microtubule plus end to the bud cortex when a productive contact site is encountered. Dynein then becomes anchored and activated to allow force generation between the microtubule and the cortex. The microtubule is pulled to slide along the cortex, causing the spindle to move into the mother-bud neck.

Our results here indicate that IC/Pac11 is necessary for HC/Dyn1 protein stability and hence dynein localization at the plus end, which is one necessary component of dynein function in the model. On the other hand, LIC/Dyn3 is not necessary for dynein targeting to the plus end, and thus must be necessary for some other process. In *dyn3*Δ cells, Dyn1-3GFP localization to the plus end is normal, but cortical Dyn1-3GFP dots were absent. Cells lacking the cortical attachment protein Num1 or dynactin show a similar phenotype, with dynein targeted to plus ends but not offloaded (Lee et al., 2003). We hypothesize that, during interaction of the plus end with the cortical attachment site, Dyn3 helps link dynein to cortical protein(s). After this interaction, Dyn3 must dissociate from the dynein motor complex because Dyn3-3YFP is not found in stationary dots at the cortex.

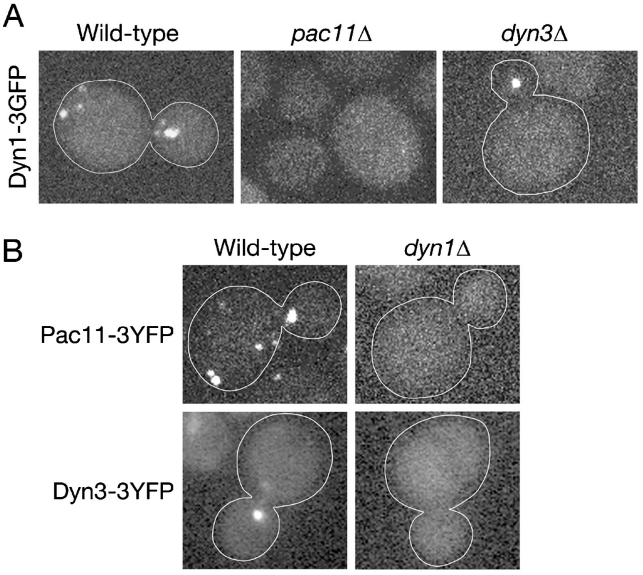

Figure 5. **Localization dependence of Dyn1-3GFP, Pac11-3YFP, and Dyn3-3YFP.** (A) 2D projection of a Z-stack of confocal images of Dyn1-3GFP in living wild-type, *pac11*Δ, and *dyn3*Δ cells. Wild-type and *dyn3*Δ cells showed Dyn1-3GFP motile dots in the bud. *pac11*Δ cells showed the absence of Dyn1-3GFP motile dots. See Videos 7–8 (available at http://www.jcb.org/cgi/content/full/jcb.200407036/DC1). (B) 2D projection of a Z-stack of confocal images of Pac11-3YFP (top row) and wide-field fluorescence images of Dyn3-3YFP (bottom row) in living wild-type and *dyn1*Δ cells. *dyn1*Δ cells showed no focal accumulations of Pac11-3YFP or Dyn3-3YFP.

To date, studies in other systems have revealed similar functions for dynein HC, IC, and LIC (Pfister et al., 1996a,b; Gaglio et al., 1997; Nurminsky et al., 1998; Compton, 2000; Tynan et al., 2000; Yoder and Han, 2001; Rusan et al., 2002; Zhang et al., 2002). Here, we describe the first clear case of differential roles of dynein subunits in cytoplasmic dynein function. Our results show that LIC functions differently from HC and IC. We find that IC, but not LIC, is needed for HC stability and localization. IC localizes to stationary cortical dots, along with HC, whereas LIC does not.

Previous biochemical work on vertebrate cytoplasmic dynein showed that separation of IC or LIC from the dynein molecule causes the HC to be unstable (King et al., 2002). In addition, vertebrate LIC associates tightly with HC and therefore appears to be a critical structural component of the dynein motor. Our findings suggest that yeast LIC is not a structural component of the dynein motor in that HC is stable in vivo in the absence of LIC. Vertebrate LIC also functions in cargo binding via direct binding to the centrosomal protein pericentrin (Purohit et al., 1999; Tynan et al., 2000). In yeast, the only "cargo" for dynein is the cell cortex. The absence of LIC at the cortex, in contrast to HC and IC, does not support a role for LIC in cargo binding.

Materials and methods

Nuclear segregation cold assay

Cultures grown to mid-log phase at 30°C in YPD were diluted 1:50 into fresh YPD and grew at 12°C to mid-log phase, which required 24–36 h. Cells were fixed with 70% ethanol, washed with 0.1 M potassium phosphate, pH 7.0, stained with DAPI, and imaged. To calculate the percentage of binucleate cells, the number of cells with two nuclei in the mother was divided by the total number of cells.

Cell lysis and immunoprecipitation

Cells were grown to mid-log phase and lysed as described previously (Lee et al., 2003). Packed cells were suspended in equal volumes of glass beads and buffer (20 mM Tris, pH 8.0, 150 mM NaCl, 10 mM EDTA, 1 mM DTT, 0.2% Triton X-100, and 1 mM PMSF, plus protease inhibitor cocktail tablet [Roche]) before lysis. Cell extracts were clarified at 100,000 *g* for 30 min. For immunoprecipitation of Dyn3-TAP, 50–75 μl of protein A beads (Amersham Biosciences) were preincubated with 35 μg/ml rabbit IgG (Cappel ICN) overnight at 4°C in 1 ml PBS. Protein A beads with bound IgG were washed four times with PBS and then incubated for 3 h at 4°C with clarified extract from *DYN1-Myc DYN3-TAP* strain (YJC3711). The beads were washed five times with lysis buffer. Bound proteins were eluted with gel sample buffer, separated with a 4% SDS gel, transferred to nitrocellulose, and immunoblotted with anti-Myc antibody (mouse 9E10 raw ascites; Covance). Protein A beads without bound IgG were used in parallel as a negative control. For immunoprecipitation of Dyn1-Myc, we incubated clarified extract from *DYN1-Myc DYN3-TAP* strain (YJC3711) with beads containing covalently bound mouse anti-Myc antibodies (9E10; Covance). Bound proteins were eluted with 0.2 M glycine, pH 2.8, separated on a 10% SDS gel, and immunoblotted with rabbit IgG that binds IgG-binding domain of TAP. An extract from a *DYN3-TAP* strain (YJC3710) in which Dyn1 was not tagged was used as a negative control. We immunoblotted to detect the Myc tag using mouse 9E10 raw ascites (Covance) and HRP-conjugated goat anti–mouse antibody at 1:2,000 and 1:10,000 dilutions, respectively. We immunoblotted to detect the TAP tag using rabbit IgG (Cappel ICN) and HRP-conjugated goat anti–rabbit antibody at 1:2,000 and 1:10,000 dilutions, respectively.

Fluorescence microscopy

Still images and movies of Pac11-3YFP or Dyn3-3YFP in mid-log phase cells were collected using NIH Image or QED software with a cooled CCD camera (Dage-MTI or Photometric CoolSNAP HQ) as described previously (Lee et al., 2003). We measured fluorescence intensity using NIH Image (Lee et al., 2003). CFP-Tub1 was used to visualize microtubules as described previously (Lee et al., 2003). Colocalization of Pac11-3YFP or Dyn3-3YFP with CFP-Tub1 was made using a single multipass dichroic filter (86002bs v1; Chroma Technology Corp.) with excitation and emission filters on motorized wheels (Ludl). Excitation filters were S500/20 and S436/10 for YFP and CFP, respectively, whereas emission filters were S535/30 and S470/30 (Chroma Technology Corp.). 3D image reconstructions of cells were prepared by collecting 0.2-μm slices using a spinning disk confocal microscope equipped with a Z-axis stage driver (MFC-2000; Applied Scientific Instruments) as described previously (Castillon et al., 2003).

Image acquisition and manipulation information

Still images or videos were acquired with a PlanApo 100× 1.4 NA objective on a fluorescence microscope (BX60; Olympus) equipped with a Photometric CoolSNAP HQ camera or a Dage-MTI cooled CCD camera. 3D images of cells were made by collecting 0.2-μm slices using a spinning disk confocal microscope equipped with a Z-axis stage driver (MFC-2000; Applied Scientific Instruments). QED software or NIH Image was used for controlling the camera and collecting images. Images were subsequently processed for brightness and contrast using Adobe Photoshop. 3D stacked images were projected using NIH Image (without replicating neighboring slices) and saved as 3D rotating videos.

Mid-log cells were grown in rich or selective synthetic defined media, washed with nonfluorescent media, and visualized directly on an agarose pad containing nonfluorescent media on a microscope slide at RT (Lee et al., 2003). CFP-Tub1 was used to visualize microtubules. Dynein complex components were labeled with a 3GFP, 3YFP, or 3CFP fluorescent tag for visualization of their localization in live cells.

Online supplemental material

The online version of this article includes additional figures showing sequence alignment and phylogenetic analysis of Dyn3 with LICs, time-lapse movies, and 3D image reconstructions of Dyn1-3GFP, Pac11-3YFP, and Dyn3-3YFP localization, as well as supplemental materials and methods. Online supplemental material available at http://www.jcb.org/cgi/content/full/jcb.200407036/DC1.

We thank Scott Bevan for dedicated technical assistance, and Dr. Rick Heil-Chapdelaine for advice and assistance with fluorescence microscopy.

Wei-Lih Lee was supported by a Damon Runyon Cancer Research Foundation Fellowship (DRG-1671). J.A. Cooper was supported by a National Institutes of Health grant (GM 47337).

Submitted: 7 July 2004
Accepted: 24 November 2004

References

Adames, N.R., and J.A. Cooper. 2000. Microtubule interactions with the cell cortex causing nuclear movements in *Saccharomyces cerevisiae*. *J. Cell Biol.* 149:863–874.

Castillon, G.A., N.R. Adames, C.H. Rosello, H.S. Seidel, M.S. Longtine, J.A. Cooper, and R.A. Heil-Chapdelaine. 2003. Septins have a dual role in controlling mitotic exit in budding yeast. *Curr. Biol.* 13:654–658.

Compton, D.A. 2000. Spindle assembly in animal cells. *Annu. Rev. Biochem.* 69:95–114.

Gaglio, T., M.A. Dionne, and D.A. Compton. 1997. Mitotic spindle poles are organized by structural and motor proteins in addition to centrosomes. *J. Cell Biol.* 138:1055–1066.

Geiser, J.R., E.J. Schott, T.J. Kingsbury, N.B. Cole, L.J. Totis, G. Bhattacharyya, L. He, and M.A. Hoyt. 1997. *Saccharomyces cerevisiae* genes required in the absence of the *CIN8*-encoded spindle motor act in functionally diverse mitotic pathways. *Mol. Biol. Cell.* 8:1035–1050.

Kahana, J.A., G. Schlenstedt, D.M. Evanchuk, J.R. Geiser, M.A. Hoyt, and P.A. Silver. 1998. The yeast dynactin complex is involved in partitioning the mitotic spindle between mother and daughter cells during anaphase B. *Mol. Biol. Cell.* 9:1741–1756.

King, S.J., M. Bonilla, M.E. Rodgers, and T.A. Schroer. 2002. Subunit organization in cytoplasmic dynein subcomplexes. *Protein Sci.* 11:1239–1250.

Lee, L., S.K. Klee, M. Evangelista, C. Boone, and D. Pellman. 1999. Control of mitotic spindle position by the *Saccharomyces cerevisiae* formin Bni1p. *J. Cell Biol.* 144:947–961.

Lee, W.L., J.R. Oberle, and J.A. Cooper. 2003. The role of the lissencephaly protein Pac1 during nuclear migration in budding yeast. *J. Cell Biol.* 160:355–364.

Miller, R.K., and M.D. Rose. 1998. Kar9p is a novel cortical protein required for cytoplasmic microtubule orientation in yeast. *J. Cell Biol.* 140:377–390.

Miller, R.K., D. Matheos, and M.D. Rose. 1999. The cortical localization of the microtubule orientation protein, Kar9p, is dependent upon actin and proteins required for polarization. *J. Cell Biol.* 144:963–975.

Nurminsky, D.I., M.V. Nurminskaya, E.V. Benevolenskaya, Y.Y. Shevelyov, D.L. Hartl, and V.A. Gvozdev. 1998. Cytoplasmic dynein intermediate-chain isoforms with different targeting properties created by tissue-specific alternative splicing. *Mol. Cell. Biol.* 18:6816–6825.

Pfister, K.K., M.W. Salata, J.F. Dillman III, E. Torre, and R.J. Lye. 1996a. Identification and developmental regulation of a neuron-specific subunit of cytoplasmic dynein. *Mol. Biol. Cell.* 7:331–343.

Pfister, K.K., M.W. Salata, J.F. Dillman III, K.T. Vaughan, R.B. Vallee, E. Torre, and R.J. Lye. 1996b. Differential expression and phosphorylation of the 74-kDa intermediate chains of cytoplasmic dynein in cultured neurons and glia. *J. Biol. Chem.* 271:1687–1694.

Purohit, A., S.H. Tynan, R. Vallee, and S.J. Doxsey. 1999. Direct interaction of pericentrin with cytoplasmic dynein light intermediate chain contributes to mitotic spindle organization. *J. Cell Biol.* 147:481–492.

Reck-Peterson, S.L., and R.D. Vale. 2004. Molecular dissection of the roles of nucleotide binding and hydrolysis in dynein's AAA domains in *Saccharomyces cerevisiae*. *Proc. Natl. Acad. Sci. USA.* 101:1491–1495.

Rusan, N.M., U.S. Tulu, C. Fagerstrom, and P. Wadsworth. 2002. Reorganization of the microtubule array in prophase/prometaphase requires cytoplasmic dynein-dependent microtubule transport. *J. Cell Biol.* 158:997–1003.

Sheeman, B., P. Carvalho, I. Sagot, J. Geiser, D. Kho, M.A. Hoyt, and D. Pellman. 2003. Determinants of *S. cerevisiae* dynein localization and activation: implications for the mechanism of spindle positioning. *Curr. Biol.* 13:364–372.

Tong, A.H., G. Lesage, G.D. Bader, H. Ding, H. Xu, X. Xin, J. Young, G.F. Berriz, R.L. Brost, M. Chang, et al. 2004. Global mapping of the yeast genetic interaction network. *Science.* 303:808–813.

Tynan, S.H., A. Purohit, S.J. Doxsey, and R.B. Vallee. 2000. Light intermediate chain 1 defines a functional subfraction of cytoplasmic dynein which binds to pericentrin. *J. Biol. Chem.* 275:32763–32768.

Yoder, J.H., and M. Han. 2001. Cytoplasmic dynein light intermediate chain is required for discrete aspects of mitosis in *Caenorhabditis elegans. Mol. Biol. Cell.* 12:2921–2933.

Zhang, J., G. Han, and X. Xiang. 2002. Cytoplasmic dynein intermediate chain and heavy chain are dependent upon each other for microtubule end localization in *Aspergillus nidulans. Mol. Microbiol.* 44:381–392.